Available online at www.sciencedirect.com
ScienceDirect
Journal of Sound and Vibration 312 (2008) 296–315
JOURNAL OF SOUND AND VIBRATION
www.elsevier.com/locate/jsvi

Nonlinear dual-axis biodynamic response of the semi-supine human body during vertical whole-body vibration

Ya Huang, Michael J. Griffin*

Human Factors Research Unit, Institute of Sound and Vibration Research, University of Southampton, Southampton SO17 1BJ, UK

Received 1 November 2006; received in revised form 18 October 2007; accepted 23 October 2007
Available online 11 December 2007

Abstract

Nonlinear biodynamic responses are evident in many studies of the apparent masses of sitting and standing subjects in static postures that require muscle activity for postural control. In the present study, 12 male subjects adopted a relaxed semi-supine posture assumed to involve less muscle activity than during static sitting and standing. The supine subjects were exposed to two types of vertical vibration (in the x-axis of the semi-supine body): (i) continuous random vibration (0.25–20 Hz) at five magnitudes (0.125, 0.25, 0.5, 0.75, and 1.0 m s^{-2} rms); (ii) intermittent random vibration (0.25–20 Hz) alternately at 0.25 and 1.0 m s^{-2} rms. With continuous random vibration, the dominant primary resonance frequency in the median normalised apparent mass decreased from 10.35 to 7.32 Hz as the vibration magnitude increased from 0.125 to 1.0 m s^{-2} rms. This nonlinear response was apparent in both the vertical (x-axis) apparent mass and in the horizontal (z-axis) cross-axis apparent mass. As the vibration magnitude increased from 0.25 to 1.0 m s^{-2} rms, the median resonance frequency of the apparent mass with intermittent random vibration decreased from 9.28 to 8.06 Hz whereas, over the same range of magnitudes with continuous random vibration, the resonance frequency decreased from 9.62 to 7.81 Hz. The median change in the resonance frequency (between 0.25 and 1.0 m s^{-2} rms) was 1.37 Hz with the intermittent random vibration and 1.71 with the continuous random vibration. With the intermittent vibration, the resonance frequency was higher at the high magnitude and lower at the low magnitude than with continuous vibration of the same magnitudes. The response was typical of thixotropy that may be a primary cause of the nonlinear biodynamic responses to whole-body vibration.

1. Introduction

Biodynamic responses of the human body to whole-body vibration are nonlinear: the resonance frequencies in frequency response functions (e.g., the apparent mass) decrease with increasing vibration magnitude. This nonlinearity has been observed in the vertical and the fore-and-aft responses of the seated human body exposed to vertical whole-body vibration (e.g. Refs. [1–5]), in the fore-and-aft and the vertical responses to the seated human body exposed to fore-and-aft whole-body vibration [6–10], and in the vertical and the fore-and-aft responses of the standing human body exposed to vertical whole-body vibration [11,12].

*Corresponding author. Tel.: +44 23 8059 2277; fax: +44 23 8059 2927.
E-mail address: M.J.Griffin@soton.ac.uk (M.J. Griffin).

0022-460X/$ - see front matter © 2007 Elsevier Ltd. All rights reserved.
doi:10.1016/j.jsv.2007.10.046

To identify factors influencing the nonlinearity, the effects of various steady-state sitting conditions have been studied, but the nonlinearity has been found in all sitting postures investigated. Increased constant muscle tension at some locations of the body had no significant effect on the nonlinearity [3,13] and there are insignificant changes in the nonlinearity with different contact pressures on the buttocks [5,9].

Electromyographic (EMG) measurements show that muscle activity in the back varies with vibration magnitude [14,15]. It has been found that voluntary periodic upper-body movement can greatly reduce the nonlinearity in the vertical apparent mass resonance frequency of the seated body [16]. With voluntary movements, the resonance frequency was 4.7 Hz at 0.25 m s^{-2} rms and 4.6 Hz at 2.0 m s^{-2} rms, whereas the resonance frequency was 5.5 Hz at 0.25 m s^{-2} rms and 4.4 Hz at 2.0 m s^{-2} rms without voluntary movement. The authors suggested that the reduction in the nonlinearity might be due to a change in the involuntary phasic activity of the muscles stimulated by the whole-body vibration when the muscles are contracted voluntarily by the periodic upper-body movement. Alternatively, both the voluntary body movement and the associated muscular contraction may have altered the dynamic stiffness of the body by changes in the passive thixotropic behaviour of the tissues.

Fairley and Griffin [1] speculated that the nonlinear loosening effect of the musculo-skeletal structure had a similar mechanism to the thixotropic property of relaxed human muscles. ‘Thixotropy’ has been used to describe a passive property of human tissues: the stiffness of tissues decreases with prior perturbation, while the stiffness increases with prior stillness or low magnitude stimuli: the dynamic stiffness of tissues depends on the immediate ‘shear history’. Following a perturbation applied to the relaxed finger extensor, the stiffness increased back to normal after a recovery time of between 5 and 10 s [17]. This thixotropic behaviour has been found in different parts of the human body: passive movement of the human wrist [18], finger extensor [17] and finger flexor [17,19]. Homma and Hagbarth [20] found that the rib cage respiratory muscles exhibit thixotropic properties similar to those observed in other skeletal muscles.

Considering the ubiquity of the nonlinearity with different sitting conditions and the prevalent thixotropic property of different parts of the body, it may be hypothesised that the intrinsic passive thixotropy of local body parts accumulatively produces the previously observed whole-body nonlinearity.

An intermittent stimulus with alternately high magnitudes and low magnitudes can be used to investigate the effect of shear history on the dynamic response of the body. Mansfield [21] found no significant difference between the resonance frequencies of apparent masses measured with continuous random vibration and alternately high–low vibration at 0.2 and 2.0 m s^{-2} rms. This may have been because the durations of the high and low magnitudes were 60 s and far longer than the recovery time of relaxed muscles and other tissues. Immediately after a tap perturbation, the stiffness of relaxed finger muscles recovered by 80% in only a couple of seconds [17].

A relaxed semi-supine posture will involve less, or at least different, trunk muscle activity than sitting and standing postures. Measuring responses in a relaxed semi-supine position may therefore allow analysis of the nonlinearity with minimal muscle activity. The primary resonance frequency in the mechanical impedance of the semi-supine human body during vertical excitation has been found near 6 Hz with both 2–20 Hz sinusoidal vibration at 3.5 m s^{-2} rms [22] and 1–20 Hz sinusoidal vibration at 2.1 m s^{-2} rms [23]. With 0.69 m s^{-2} peak-to-peak sinusoidal vibration between 2 and 20 Hz, the resonance was reported to be around 5 Hz for transmissibility to the chest, and 5–11 Hz for transmissibility to the abdomen of supine subjects [24]. With semi-supine space crew, the primary resonance frequency of the mechanical impedance was observed between 7 and 11 Hz during 1–70 Hz sinusoidal vibration at 2.8 m s^{-2} rms [25]. The variation in resonance frequency between these studies might be due to differences in the magnitudes of vibration, variations in the supine postures, the measuring locations, the frequency resolutions, and inter-subject variability. Most of these studies were conducted with a single magnitude of vibration and some with a sustained acceleration.

It is not known whether with vertical excitation of subjects in a relaxed semi-supine posture the ‘in-line’ dynamic response is as nonlinear as in sitting and standing postures, or whether the nonlinearity will be present in the horizontal cross-axis direction in the mid-sagittal plane of the body.

It was hypothesised that, in a relaxed semi-supine posture, both the vertical apparent mass resonance frequencies and the longitudinal horizontal cross-axis apparent mass peak frequencies would decrease with increasing vibration magnitude. It was also hypothesised that with random vibration consisting of intermittent periods at a low magnitude (0.25 m s^{-2} rms) and a high magnitude (1.0 m s^{-2} rms) the stiffness of the body would be decreased by prior high magnitude vibration and increased by prior low magnitude vibration, so reducing and raising, respectively, the resonance frequency.

2. Method

2.1. Apparatus

A supine support was constructed with three parts: back support, leg rest, and headrest (Fig. 1).

The back support was a horizontal flat rigid 660 mm × 660 mm × 10 mm aluminium plate with a high stiffness 3 mm thick laterally treaded rubber layer attached to the upper surface. The complete back support was bolted rigidly to the upper surface of the force platform, which monitored the vertical (x-axis of the semi-supine subject) and horizontal (z-axis of the semi-supine subject) forces exerted by the subject on the back support. The force platform was bolted rigidly to the vibrator platform. The horizontal distance between the edge of the back support and the edge of the leg rest was 50 mm (Fig. 1).

The legs of subjects rested on a horizontal flat rigid aluminium support with an 8-mm thick high stiffness rubber layer attached to the top. The height of the leg rest was adjusted to allow the lower legs to rest horizontally.

The headrest was a horizontal flat rigid wooden block with 75-mm thick car-seat foam attached to the upper surface. The top surface of the complete headrest was approximately 50 mm higher than the back support. The horizontal distance between the back support and the headrest was adjusted by moving the headrest so that a subject's head could rest comfortably.

Vertical vibration was produced by a 1-m stroke electro-hydraulic vertical vibrator capable of accelerations up to $\pm 10\,\mathrm{m\,s^{-2}}$ in the laboratory of the Human Factors Research Unit.

The vertical (x-axis) and the horizontal (z-axis) accelerations of the vibrator platform were measured using two identical Setra 141A $\pm 2g$ accelerometers fixed on the plane of vibrator platform below the back support and between the leg rest and the force platform (Fig. 1). The vertical (x-axis) and the horizontal (z-axis) forces at the back support were measured using a Kistler 9281 B21 12-channel force platform. The four vertical (x-axis) force signals and the four horizontal (z-axis) force signals from the four corners of the platform were summed and conditioned using two Kistler 5001 charge amplifiers.

An *HVLab* v3.81 data acquisition and analysis system was used to generate test stimuli and acquire the vertical and horizontal accelerations and the vertical and horizontal forces from the transducers. The two acceleration signals and the two force signals were acquired at 200 samples per second via 67 Hz analogue anti-aliasing filters.

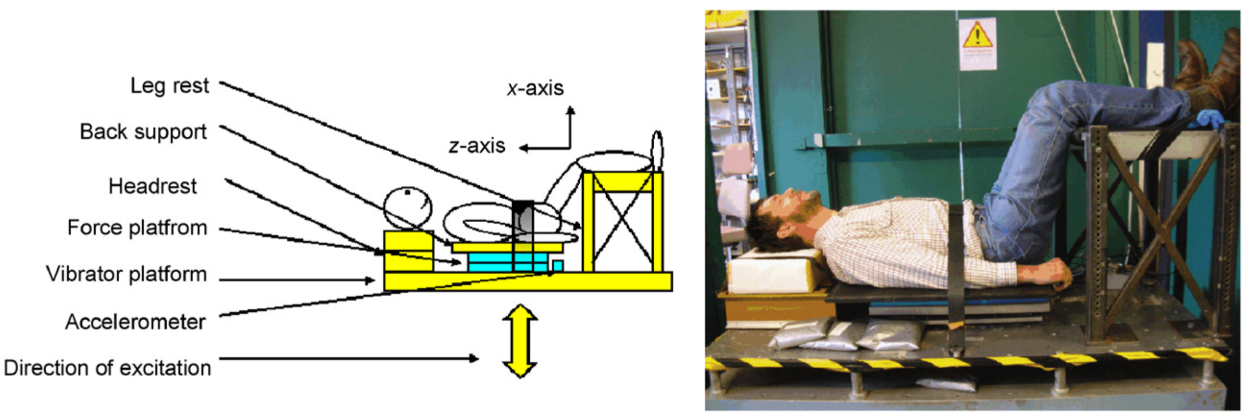

Fig. 1. Schematic diagram of the supine support showing the semi-supine position and the axes of the force (z- and x-axis) and the acceleration (x-axis) transducers. A photographic representation of a test subject in the relaxed semi-supine position for vertical whole-body vibration.

2.2. Stimuli

The random stimuli used in this study had approximately flat constant-bandwidth acceleration power spectra over the frequency range 0.25–20 Hz.

Two types of vertical vibration were employed:

(i) Continuous random vibration with a duration of 90 s tapered at the start and end with 0.5-s cosine tapers. Five accelerations at 0.125, 0.25, 0.5, 0.75, and 1.0 $m\,s^{-2}$ rms (unweighted) were generated using different random seeds (giving different time histories). Twelve subjects were randomly divided into six groups with two persons per group. With different groups, different random seeds were used to generate the random stimuli.
(ii) Intermittent random vibration, alternately at 0.25 and 1.0 $m\,s^{-2}$ rms (unweighted) with a total duration of 828 s. The 828-s intermittent stimulus was divided evenly into four identical 207-s sections (Fig. 2a). During each 207-s section, 18 high magnitude slices and 18 low magnitude slices (generated using different random seeds) were presented alternately. The duration of 828 s was determined so that there were sufficient high magnitude and low magnitude slices for the concatenated signals (at high or low magnitude) to have the same duration as each of the continuous signals (i.e., 90 s). One single cycle of the intermittent signal was defined as one high magnitude slice followed by one low magnitude slice. During a single cycle of the intermittent motion, the high magnitude slice (at 1.0 $m\,s^{-2}$ rms) lasted for 6 s (tapered at the start and end with a 0.25-s cosine taper) followed by a low magnitude slice (at 0.25 $m\,s^{-2}$ rms) for 5.5 s (Fig. 2b). The durations of the high or low magnitude slices were determined so that the effective high or low magnitude signals (after removing the tapering) could be analysed with a frequency resolution of about 0.4 Hz (see Section 2.5.2).

All test motions were presented in one session lasting approximately 100 min. The order of presentation of the six random stimuli (the continuous stimuli at five magnitudes and the intermittent stimulus) was balanced across the 12 subjects.

2.3. Posture

While experiencing each motion, subjects maintained a relaxed semi-supine position with their lower legs lifted and resting on the horizontal leg rest so as to give maximum back contact with the back support (Fig. 1). The horizontal distance between the bottom of buttocks (aligned with the edge of the back support) and the near edge of the leg rest was 50 mm for all subjects. Subjects were instructed to relax totally with their eyes closed. A loose safety belt passed around the subject abdomen and arms but did not constrain the body.

2.4. Subjects

Twelve male subjects, aged between 20 and 42 years, with median (minimum and maximum) stature 1.73 m (1.66 and 1.80 m) and median total body mass 66.4 kg (58.3 and 86.2 kg) participated in the study.

The experiment was approved by the Human Experimentation, Safety and Ethics Committee of the Institute of Sound and Vibration Research at the University of Southampton.

2.5. Analysis

2.5.1. Continuous random vibration

The vertical (x-axis) and horizontal (z-axis) forces measured at the supine back support were analysed relative to the vertical (x-axis) acceleration (Fig. 1). Two frequency response functions—apparent mass (where the force was in-line with the acceleration in the vertical direction) and horizontal cross-axis apparent mass (where the horizontal force was perpendicular to the vertical acceleration in the sagittal plane, i.e. the z-axis)—were calculated using the cross-spectral density method:

$$M(f) = S_{af}(f)/S_{aa}(f), \tag{1}$$

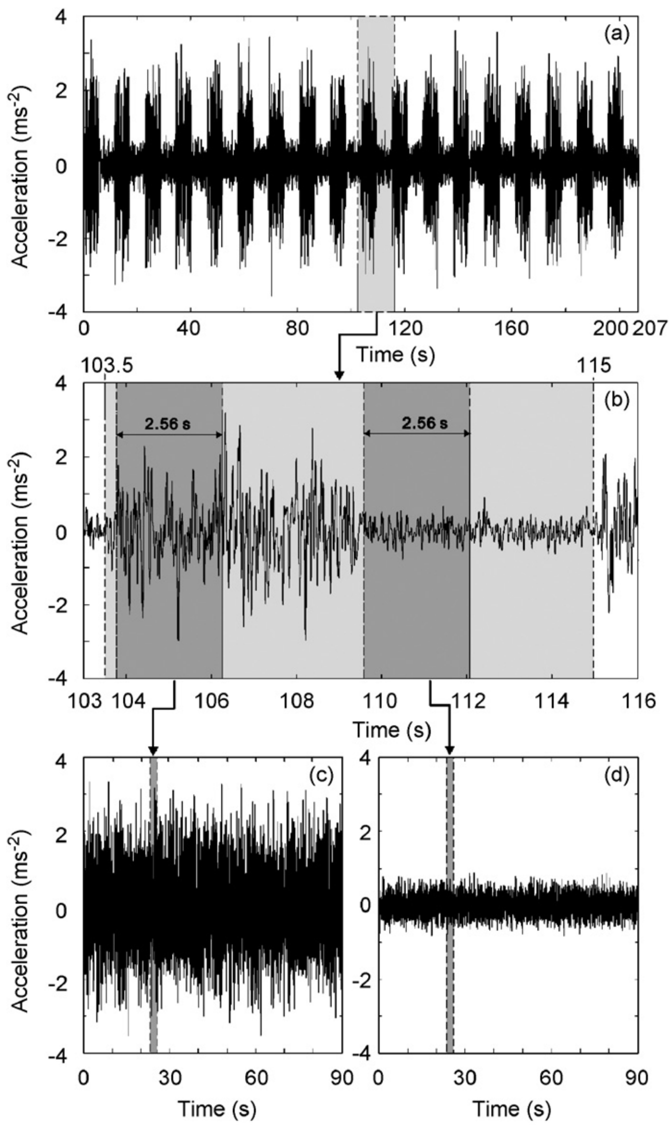

Fig. 2. An example of a vertical input acceleration time history measured with the high–low (1.0–0.25 m s^{-2} rms) magnitude intermittent random stimuli showing: (a) one complete 207-s intermittent time history; (b) one period of the intermittent time history starting with 6-s high magnitude slice followed by a 5.5-s low magnitude slice; (c) extracted and catenated high magnitude (1.0 m s^{-2} rms) time slices (2.56 s each); (d) extracted and catenated low magnitude (0.25 m s^{-2} rms) time slices (2.56 s each). The same procedure was applied to vertical force and horizontal cross-axis force time histories.

where $M(f)$ is the vertical apparent mass or the horizontal z-axis cross-axis apparent mass, in kg, $S_{af}(f)$ the cross-spectral density between the measured forces and the vertical excitation acceleration, and $S_{aa}(f)$ the power spectral density of the vertical excitation acceleration.

Before calculating the vertical apparent mass, mass cancellation (of the equipment above the force sensing elements) was carried out in the time domain to subtract the force caused by the masses above the force sensing elements (a total of 30.5 kg obtained dynamically in the frequency range 0.25–20 Hz). No mass cancellation was needed to calculate the horizontal cross-axis apparent mass as there was no input motion in this direction.

The apparent masses at the five magnitudes were normalised by dividing by the apparent mass modulus measured at frequencies between 0.25 and 1.5 Hz, where the body was considered rigid. For motion at

$0.125\,\mathrm{m\,s^{-2}}$ rms, the normalisation was carried out at 1.37 Hz, for $0.25\,\mathrm{m\,s^{-2}}$ rms at 1.37 Hz, for $0.5\,\mathrm{m\,s^{-2}}$ rms at 0.59 Hz, for $0.75\,\mathrm{m\,s^{-2}}$ rms at 0.59 Hz, for $1.0\,\mathrm{m\,s^{-2}}$ rms at 0.39 Hz. The median normalised apparent masses at the five magnitudes were then calculated. The horizontal z-axis cross-axis apparent masses at the five magnitudes were normalised by dividing by the vertical apparent mass modulus measured at the same frequencies as the vertical apparent mass at each magnitude. The median normalised z-axis cross-axis apparent masses were then calculated.

The cross-spectral densities and the power spectral densities were both estimated via Welch's method at frequencies between 0.25 and 20 Hz. The frequency response functions for each of the 90-s continuous random signals used a fast Fourier transform windowing length of 2048 samples, a hamming window with 100% overlap, a sampling rate of 200 samples per second and an ensuing frequency resolution of 0.10 Hz. This signal processing procedure applied to signals measured with continuous vibration is referred as the 0.1-Hz procedure.

2.5.2. Intermittent random vibration

Before the intermittent signals (vertical acceleration excitation, vertical force, and horizontal force) were analysed according to the procedure applied to the continuous signals (Section 2.5.1), the intermittent signals described in Section 2.2 (ii) were processed as follows.

Each of the high magnitude ($1.0\,\mathrm{m\,s^{-2}}$ rms) and low magnitude ($0.25\,\mathrm{m\,s^{-2}}$ rms) time slices of the accelerations and forces measured with each of the 828-s intermittent signals was extracted and concatenated into a processed high magnitude signal (90 s duration) and a processed low magnitude signal (90 s duration) (Fig. 2C and D). The duration of each extracted time slice was 2.56 s to allow the apparent masses to be measured and calculated before the dynamic stiffness of the body recovered from the prior immediate high magnitude or low magnitude vibration. Each of the force and acceleration time histories measured with the continuous random stimuli and each of the processed force and acceleration time histories measured with the intermittent random stimuli lasted for 90 s, allowing the apparent masses to be calculated with the same frequency resolution of 0.40 Hz for both stimuli.

The same procedure used to analyse the signals measured with continuous random vibration (Section 2.2 (i)) was used to calculate the apparent masses and cross-axis apparent masses with each of the 90-s high magnitude ($1.0\,\mathrm{m\,s^{-2}}$ rms) or low magnitude ($0.25\,\mathrm{m\,s^{-2}}$ rms) processed intermittent signals, except for a different signal processing procedure (0.4-Hz procedure, Table 1). The 0.4-Hz criterion was used to generate apparent masses and cross-axis apparent masses with each of the 90-s processed intermittent acceleration and force signals. The 0.4-Hz procedure was also used to analyse accelerations and forces measured with the continuous vibration at 0.25 and $1.0\,\mathrm{m\,s^{-2}}$ rms so that the apparent masses measured with the intermittent and the continuous vibration could be compared using the same frequency resolution (0.40 Hz) with the same signal duration (90 s). Finally, the frequency resolution obtained using the 0.4-Hz procedure with both intermittent and continuous signals at 0.25 and $1.0\,\mathrm{m\,s^{-2}}$ rms was increased to 0.10 Hz by linearly interpolating the apparent mass moduli and phases in the frequency domain. The 0.4-Hz procedure used 0% overlap (with a Hamming window) to eliminate discontinuity caused by the concatenation of the 2.56-s slices.

Table 1
Two signal processing procedures used to analyse measurement with the continuous random stimuli and with the intermittent random stimuli

Duration (s)	Sampling rate (Hz)	FFT length	Degrees of freedom	Windowing overlap	Frequency resolution (Hz)
(A) 0.1-Hz procedure—for measured accelerations and forces with continuous random vibration at 0.125, 0.25, 0.5, 0.75, and $1.0\,\mathrm{m\,s^{-2}}$ *rms*					
90	200	2048	36	100%	0.10
(B) 0.4-Hz procedure—for processed accelerations and forces measured at 0.25 and $1.0\,\mathrm{m\,s^{-2}}$ *rms for both the intermittent and continuous random vibration*					
90	200	512	70	0%	0.40 (then linearly interpolated to 0.10 in the frequency domain)

2.5.3. Curve-fitting, apparent mass resonance frequencies and cross-axis apparent mass peak frequencies

A parallel two-degree-of-freedom parametric model was used to fit the vertical in-line individual apparent masses and phases in order to obtain primary resonance frequencies. This model has been found to give a good fit to the measured values of the apparent masses of 60 seated subjects [26]. To quantify the biodynamic nonlinearity, the primary resonance frequencies of both individual and median normalised apparent masses are represented here by the frequency at which the modulus of the apparent mass was a maximum in the fitted curve. Huang and Griffin [16] used the same model to quantify the nonlinearity apparent at different vibration magnitudes with 12 seated subjects.

The horizontal z-axis cross-axis apparent mass 'peak frequency' was defined as the frequency at which the modulus of the measured cross-axis apparent mass had a maximum value within a limited frequency range where coherency was reasonably high (more than 0.7). The peak frequencies were considered to be a representation of the stiffness of some parts of the body system similar to the resonance frequencies. This simplification was necessary as the z-axis cross-axis response of the body exhibited the behaviour of a multi-degree-of-freedom system with several peaks and troughs.

The curve-fitting method used a constrained minimum error search command 'fmincon()' of the optimisation toolbox of *MATLAB* (version 7.0.1, R14, SP1). The target error was calculated by summing the square of errors in modulus (kg) and phase (rad) at each frequency point between the measurement and the fitted curve. Before summation, the modulus errors were re-scaled to have an equivalent scale to the phase errors by multiplying the modulus (at each frequency point from 0.5 to 20 Hz) by a normalisation factor

$$P = |\mathrm{PH}_s|_{\max}/|\mathrm{AM}_s|_{\max}, \tag{2}$$

where $|\mathrm{AM}_s|_{\max}$ is the maximum value of the modulus of the measured apparent mass (kg) at any frequency point between 0.5 and 20 Hz, and $|\mathrm{PH}_s|_{\max}$ is the maximum absolute value of measured phase (rad). Therefore, the normalisation was based on the values at two frequencies: one giving the maximum modulus and the other giving the maximum absolute phase.

The apparent mass modulus errors were then summed over the frequency range 0.5–20 Hz. The phase errors were calculated similarly except that they were not normalised (by the factor P) but multiplied by an empirical phase weighting factor Q (given a value of 5.0) in order to produce the best fit. The overall target error (cost function) was expressed of the form

$$E = \sum_N \{P[\mathrm{AM}_m(f) - \mathrm{AM}_s(f)]^2\} + \sum_N \{Q[\mathrm{PH}_m(f) - \mathrm{PH}_s(f)]^2\}, \tag{3}$$

where E is the overall target error between the fitted curve and measured apparent masses, N is the number of frequency points in the measured apparent mass, $\mathrm{AM}_m(f)$ and $\mathrm{PH}_m(f)$ are the apparent mass modulus and phase of the model at each frequency, $\mathrm{AM}_s(f)$ and $\mathrm{PH}_s(f)$ are the measured apparent mass modulus and phase at each frequency, P the normalisation factor for apparent mass modulus, Eq. (2), $Q = 5.0$ is the phase weighting factor; f refers to the frequencies of curve fitting from 0.5 to 20 Hz.

The same curve-fitting procedure was carried out with the vertical apparent masses at the five magnitudes (0.125, 0.25, 0.5, 0.75, and 1.0 m s^{-2} rms) of continuous random vibration and the two magnitudes (0.25 and 1.0 m s^{-2} rms) of processed intermittent random vibration.

By fitting the parallel two-degree-of-freedom model to vertical in-line apparent masses with the curve-fitting procedure, the apparent mass resonance frequency (f_r), the apparent mass at resonance (AM_r), segmental masses (m_0, m_1, and m_2), stiffnesses (k_1 and k_2) and damping constants (c_1 and c_2) were obtained.

3. Results

3.1. Response in the vertical (x-axis) direction

3.1.1. Overview

The individual apparent masses and phases of 12 subjects with five vibration magnitudes of continuous random vibration are shown in Fig. 3. The median normalised apparent masses and phases of the group of 12

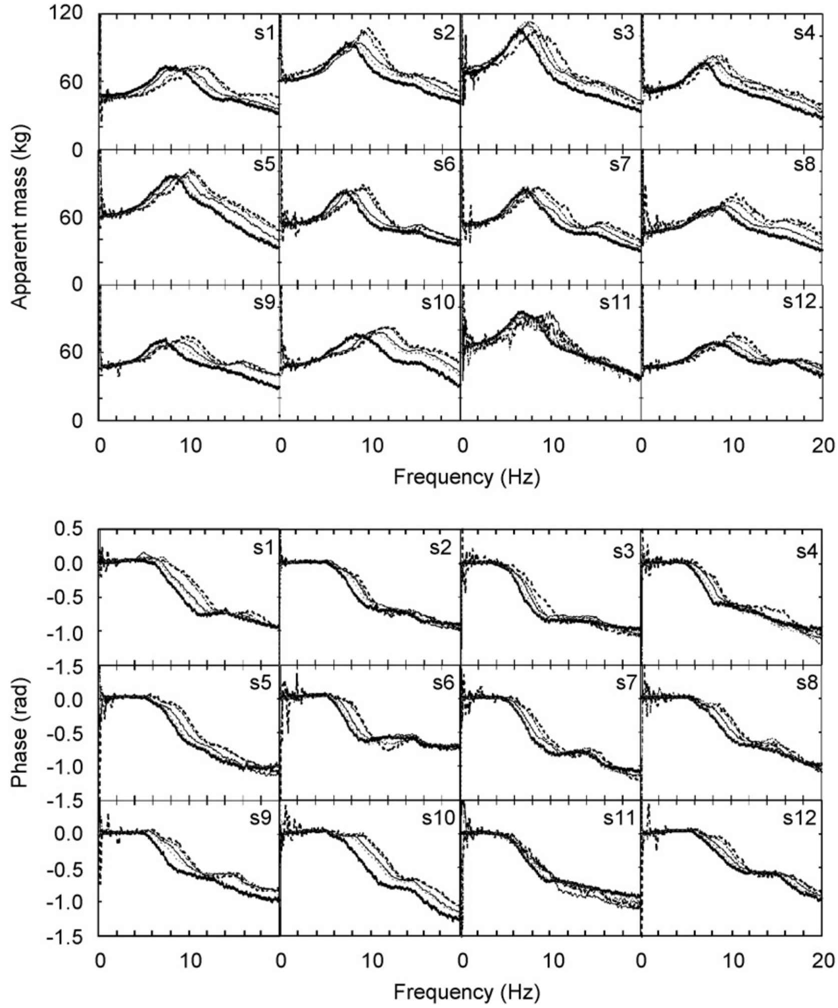

Fig. 3. Individual apparent masses (upper) and phases (lower) of 12 subjects (s1–s12) at five vibration magnitudes (- - - - - $0.125\,m\,s^{-2}$ rms; —·—·—·—·— $0.25\,m\,s^{-2}$ rms; ——— $0.5\,m\,s^{-2}$ rms; ········ $0.75\,m\,s^{-2}$ rms; ▬▬▬ $1.0\,m\,s^{-2}$ rms) of continuous random stimuli.

subjects are shown in Fig. 4. The medians and full ranges of individual apparent mass resonance frequencies are shown in Table 2. The individual apparent masses and phases of the 12 subjects at two vibration magnitudes (0.25 and $1.0\,m\,s^{-2}$ rms) with both continuous and intermittent random vibration are shown in Fig. 5.

Consistently low target errors (Eq. (3)) were obtained by curve fitting to the two-degree-of-freedom model (Fig. 6). The results of the curve fitting for the subject with the greatest fitting error (S11) is shown for five magnitudes of continuous random vibration in Fig. 7.

The lowest coherency occurred with the lowest vibration magnitude ($0.125\,m\,s^{-2}$ rms), probably due to involuntary and voluntary subject movement (e.g. breathing and stretching), mainly at frequencies less than 1.0–2.0 Hz. The coherencies were generally in excess of 0.9 in the frequency range 0.5–20 Hz.

There was one dominant primary resonance frequency of the vertical apparent mass between 6.0 and 12.0 Hz. A minor secondary resonance occurred in the frequency range 14.0–20.0 Hz, which was most distinct with subjects 1, 2, 6, 7, 8, 9, 10, and 12.

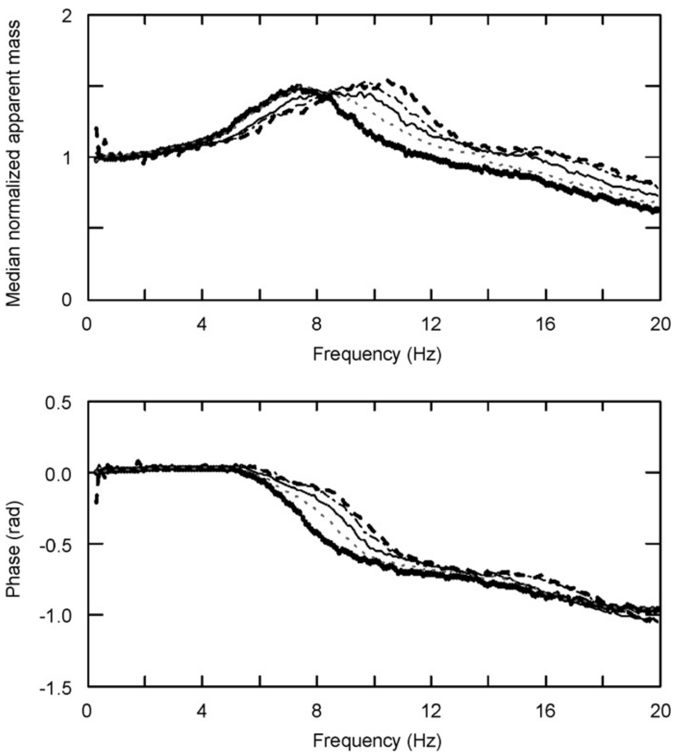

Fig. 4. Median normalised apparent masses (upper) and phases (lower) of the group of 12 subjects at five vibration magnitudes (- - - - - 0.125 m s^{-2} rms; —·—·—·—·— 0.25 m s^{-2} rms; ——— 0.5 m s^{-2} rms; ········ 0.75 m s^{-2} rms; ━━━ 1.0 m s^{-2} rms) of continuous random stimuli.

Table 2
Median and ranges of resonance frequencies of apparent masses generated by fitting the two-degree-of-freedom parametric model to the apparent masses and phases of 12 subjects at five vibration magnitudes (0.125, 0.25, 0.5, 0.75, and 1.0 m s^{-2} rms) of continuous random stimuli

Resonance frequency	Minimum	Median	Maximum
$f_{0.125}$ (Hz)	8.50	10.01	12.11
$f_{0.25}$ (Hz)	8.01	9.62	11.82
$f_{0.5}$ (Hz)	7.62	9.08	10.94
$f_{0.75}$ (Hz)	7.13	8.50	10.65
$f_{1.0}$ (Hz)	6.84	7.81	9.18

$f_{0.125}$, $f_{0.25}$, $f_{0.5}$, $f_{0.75}$, and $f_{1.0}$: resonance frequencies at five vibration magnitudes (0.125, 0.25, 0.5, 0.75, and 1.0 m s^{-2} rms).

3.1.2. *Apparent mass resonance frequencies with continuous random vibration*

The apparent mass resonance frequency decreased significantly with increasing vibration magnitude ($p<0.01$, Friedman two-way analysis of variance). There was a significant difference between each of the resonance frequencies at the five magnitudes ($p<0.01$, Wilcoxon matched-pairs signed ranks test).

The median resonance frequencies of the apparent masses of the 12 subjects decreased from 10.01 to 7.81 Hz as the vibration magnitude increased from 0.125 to 1.0 m s^{-2} rms (Table 2).

The resonance frequencies of the median normalised apparent masses (Fig. 4) of the group of 12 subjects were 10.35, 9.67, 8.01, 7.42, and 7.32 Hz with vibration magnitudes of 0.125, 0.25, 0.5, 0.75, and 1.0 m s^{-2} rms, respectively.

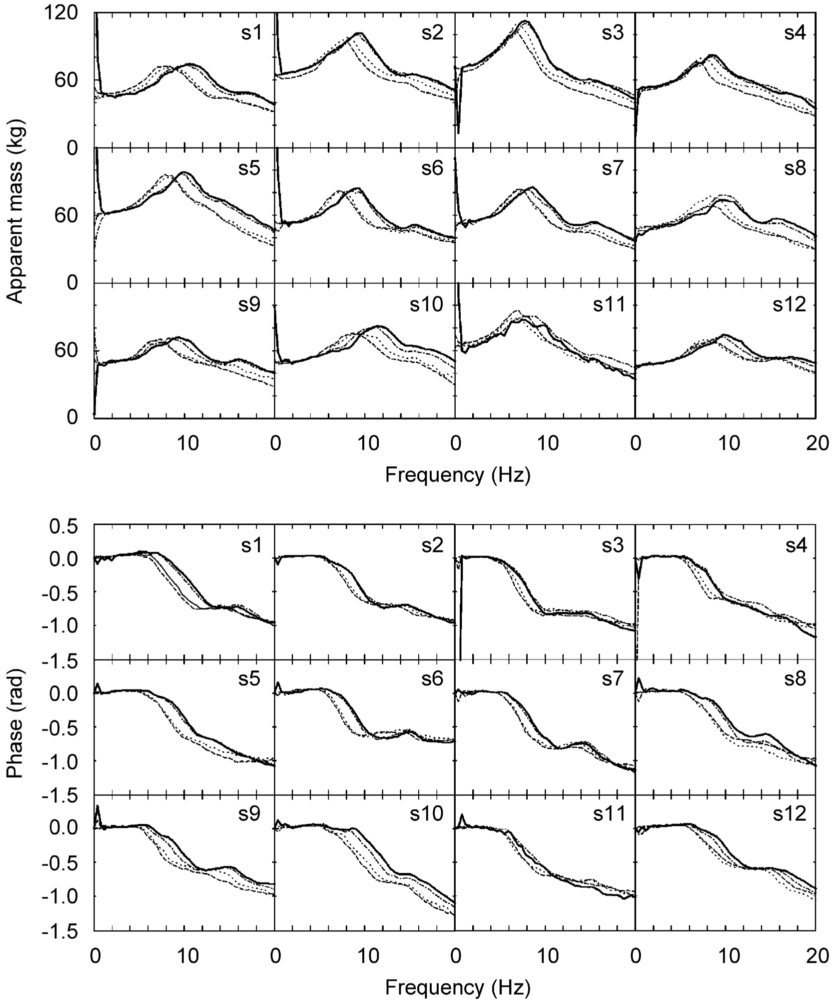

Fig. 5. Individual apparent masses (upper) and phases (lower) of 12 subjects (s1–s12) at two vibration magnitudes (— · — · — · — · — $0.25\,\mathrm{m\,s^{-2}}$ rms intermittent; ········ $1.0\,\mathrm{m\,s^{-2}}$ rms intermittent; ▬▬▬ $0.25\,\mathrm{m\,s^{-2}}$ rms continuous; - - - - - $1.0\,\mathrm{m\,s^{-2}}$ rms continuous) of both intermittent and continuous random stimuli.

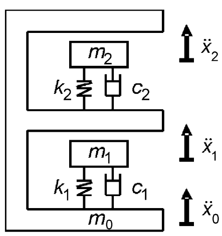

Fig. 6. Parallel two-degree-of-freedom lumped parameter model used to fit the apparent masses and phases so as to obtain resonance frequencies. The 'x-axis' is vertical excitation of semi-supine subjects.

3.1.3. Parameters of the two-degree-of-freedom model fitted to the apparent masses with continuous random vibration

The medians and ranges of the parameters of the two-degree-of-freedom model fitted to individual apparent masses and phases are shown in Table 3. The effect of vibration magnitude on the model parameters has been

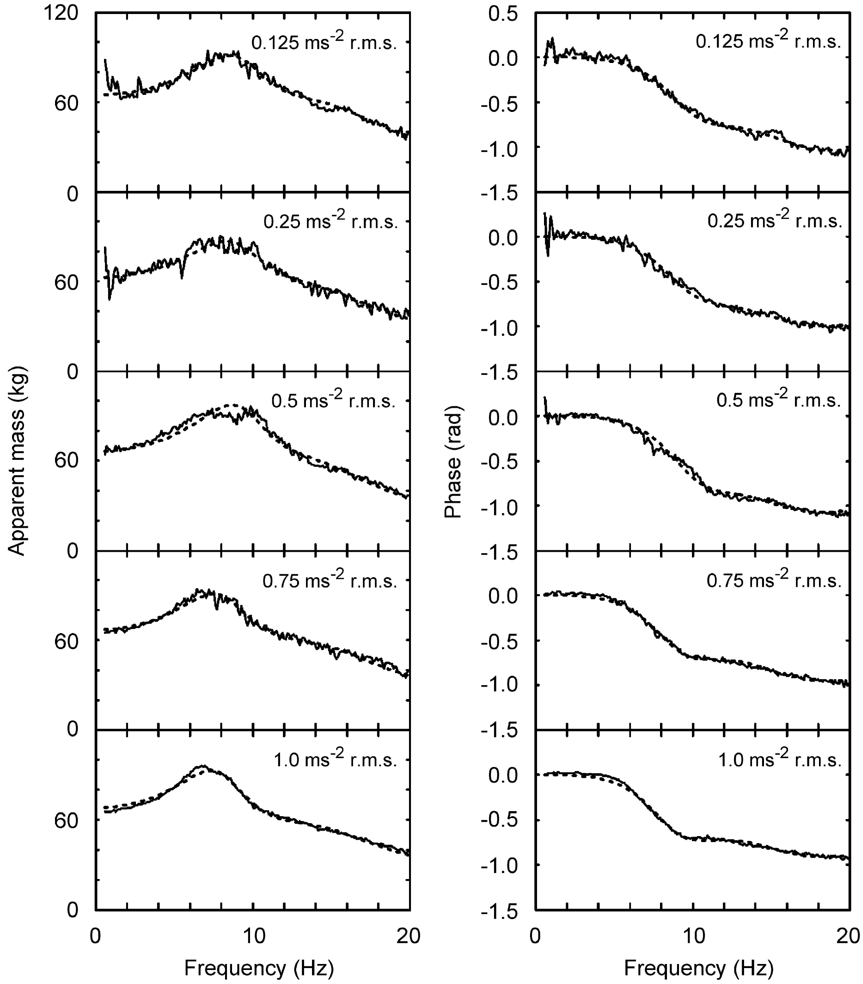

Fig. 7. An example of curve-fitting (———— measurement; - - - - - fitted curve) the apparent masses and phases of one subject (s11) at five magnitudes (0.125, 0.25, 0.5, 0.75 and 1.0 m s^{-2} rms) of continuous random stimuli to obtain the resonance frequencies (Hz). Frequency range of curve fitting: 0.5–20 Hz.

investigated. The segmental mass m_1, stiffness k_1, and damping constant c_1, correspond to the primary resonance between 6.0 and 12.0 Hz. The segmental mass m_2, stiffness k_2, and damping constant c_2, correspond to the secondary resonance between 14.0 and 20.0 Hz. The frame mass, m_0, was included to give better fitting results [26].

The five vibration magnitudes had a significant overall effect on the frame mass, m_0 ($p<0.01$, Friedman). The frame mass tended to decrease with increasing magnitude ($p<0.05$, Wilcoxon), except between 0.25 and 0.5 m s^{-2} rms ($p=0.126$, Wilcoxon), between 0.25 and 0.75 m s^{-2} rms ($p=0.239$, Wilcoxon), between 0.5 and 0.75 m s^{-2} rms ($p=0.844$, Wilcoxon), between 0.5 and 1.0 m s^{-2} rms ($p=0.071$, Wilcoxon), and between 0.75 and 1.0 m s^{-2} rms ($p=0.136$, Wilcoxon). There was no significant effect of vibration magnitude on the primary segmental mass, m_1 ($p=0.615$, Friedman) or the secondary segmental mass, m_2 ($p=0.194$, Friedman).

The vibration magnitude had an overall effect on the primary segmental stiffness, k_1 ($p<0.01$, Friedman), which tended to decrease with increasing vibration magnitude ($p<0.05$, Wilcoxon) except between 0.5 and 0.75 m s^{-2} rms ($p=0.117$, Wilcoxon), and between 0.75 and 1.0 m s^{-2} rms ($p=0.433$, Wilcoxon). The vibration magnitude also had an overall effect on the secondary segmental stiffness, k_2 ($p<0.01$, Friedman), which tended to decrease with increasing magnitude ($p<0.05$, Wilcoxon) except between 0.125 and 0.25 m s^{-2}

Table 3
Median and ranges of parameters generated by fitting the two-degree-of-freedom parametric model to the apparent masses and phases of 12 subjects at five vibration magnitudes (0.125, 0.25, 0.5, 0.75, and 1.0 $m s^{-2}$ rms) of continuous random stimuli

Vibration magnitude ($m s^{-2}$ rms)	m_0 (kg)	m_1 (kg)	k_1 ($N m^{-1}$)	c_1 ($N s m^{-1}$)	m_2 (kg)	k_2 ($N m^{-1}$)	c_2 ($N s m^{-1}$)	f_r (Hz)
0.125								
Minimum	16.5	9.5	51,876	226	9.9	10,7118	531	8.50
Median	21.2	15.0	75,373	421	17.7	226,389	1280	10.01
Maximum	25.9	32.7	125,815	1436	31.6	332,926	2193	12.11
0.25								
Minimum	13.5	9.6	47,403	210	7.9	86,288	472	8.01
Median	19.3	13.3	59,658	343	21.9	237,016	1634	9.62
Maximum	24.0	34.7	128,742	1656	32.7	351,234	2321	11.82
0.5								
Minimum	15.2	10.0	30,358	190	2.8	33,311	92	7.62
Median	18.2	12.4	54,952	332	20.6	219,720	1585	9.08
Maximum	22.8	45.0	178,344	2343	32.9	294,682	2662	10.94
0.75								
Minimum	13.6	11.7	40,154	245	18.1	166,046	1178	7.13
Median	17.7	13.4	50,844	379	20.1	193,479	1578	8.50
Maximum	22.4	28.5	71,239	835	33.8	280,341	2929	10.65
1.0								
Minimum	14.3	10.5	25,239	193	14.2	149,178	744	6.84
Median	16.9	14.8	52,365	429	21.2	163,275	1730	7.81
Maximum	22.1	27.6	81,153	708	30.6	234,006	2675	9.18

m_0, m_1, and m_2—segmental masses. k_1 and k_2—segmental stiffnesses. c_1 and c_2—segmental damping constants, and f_r—apparent mass resonance frequency of the model.

rms ($p = 0.347$, Wilcoxon), between 0.125 and 0.5 $m s^{-2}$ rms ($p = 0.136$, Wilcoxon), and between 0.125 and 0.75 $m s^{-2}$ rms ($p = 0.071$, Wilcoxon).

There was no significant effect of vibration magnitude on the primary segmental damping constant, c_1 ($p = 0.748$, Friedman) or the secondary segmental damping constant, c_2 ($p = 0.220$, Friedman).

The variations in the parameters with varying vibration magnitude allowed consistently good fits between the model and the measured apparent mass. However, the parameters are not suggested as representative of the dynamic characteristics of specific parts of the human body or differences in specific body parts between different subjects.

3.1.4. Apparent mass resonance frequencies with intermittent random vibration

As vibration magnitude increased from 0.25 to 1.0 $m s^{-2}$ rms, the median resonance frequency of the apparent mass decreased from 9.28 to 8.06 Hz with intermittent random vibration, and from 9.62 to 7.81 Hz with continuous random vibration (Table 4A).

The resonance frequencies with intermittent random vibration at 0.25 $m s^{-2}$ rms were significantly lower than those with continuous random vibration at the same magnitude ($p = 0.025$, Wilcoxon). This effect was apparent for all except subjects 3 and 11 (Table 4A and Fig. 5). The resonance frequencies with intermittent random vibration at 1.0 $m s^{-2}$ rms were significantly higher than those with continuous random vibration at the same magnitude ($p = 0.034$, Wilcoxon). This effect was apparent for all except subjects 11 and 12 (Table 4A and Fig. 5).

The absolute difference between the resonance frequencies at 0.25 and 1.0 $m s^{-2}$ rms was significantly less with intermittent random vibration than with the continuous random vibration ($p = 0.015$, Wilcoxon). This effect was present for all except subject 11 (Table 4A and Fig. 5). The median reduction in resonance

Table 4
Median and ranges of resonance frequencies and model parameters generated by fitting the two-degree-of-freedom parametric model to the apparent masses and phases of 12 subjects at two vibration magnitudes (0.25 and 1.0 $m s^{-2}$ rms) of both continuous and intermittent random stimuli

(*A*) *Resonance frequency* (*Hz*)

Subject	0.25 $m s^{-2}$ rms intermittent	0.25 $m s^{-2}$ rms continuous	1.0 $m s^{-2}$ rms intermittent	1.0 $m s^{-2}$ rms continuous
s1	10.65	11.04	9.18	8.59
s2	9.38	9.47	8.20	8.01
s3	8.01	7.91	7.23	6.84
s4	8.69	8.79	7.71	7.13
s5	9.96	10.25	8.50	8.40
s6	9.18	9.38	7.91	7.62
s7	8.40	8.79	7.52	7.42
s8	10.16	10.25	8.69	8.59
s9	8.98	9.77	7.62	7.32
s10	11.13	11.82	9.77	9.18
s11	8.50	8.20	7.03	7.32
s12	9.86	10.55	8.50	8.79
Minimum	8.01	7.91	7.03	6.84
Median	9.28	9.62	8.06	7.81
Maximum	11.13	11.82	9.77	9.18

(*B*) *Model parameters*

Vibration magnitude ($m s^{-2}$ rms)	m_0 (kg)	m_1 (kg)	k_1 ($N m^{-1}$)	c_1 ($N s m^{-1}$)	m_2 (kg)	k_2 ($N m^{-1}$)	c_2 ($N s m^{-1}$)	f_r (Hz)
0.25 intermittent								
Minimum	15.1	10.6	39,883	237	13.8	162,269	737	8.01
Median	18.8	14.4	70,758	407	19.5	232,477	1454	9.28
Maximum	24.2	28.3	106,650	1135	32.0	296,319	2864	11.13
0.25 continuous								
Minimum	13.3	9.7	47,817	223	6.7	73,096	355	7.91
Median	18.9	13.2	60,506	341	22.2	243,550	1533	9.62
Maximum	25.2	35.3	131,477	1702	32.1	352,212	2296	11.82
1.0 intermittent								
Minimum	14.8	12.4	35,956	277	13.8	141,198	847	7.03
Median	17.7	16.1	59,117	456	20.8	182,644	1669	8.06
Maximum	21.4	32.0	90,193	1326	29.9	264,476	2625	9.77
1.0 continuous								
Minimum	14.3	10.4	24,859	193	14.0	147,512	742	6.84
Median	16.9	14.9	52,442	433	21.3	161,898	1743	7.81
Maximum	22.0	27.7	82,605	720	30.3	234,212	2664	9.18

m_0, m_1, and m_2—segmental masses, k_1 and k_2—segmental stiffnesses, c_1 and c_2—segmental damping constants, and f_r—apparent mass resonance frequency of the model.

frequency between 1.0 and 0.25 $m s^{-2}$ rms was less with intermittent random vibration (1.37 Hz) than with continuous random vibration (1.71 Hz).

3.1.5. Parameters of the two-degree-of-freedom model fitted to the apparent masses with intermittent random vibration

The median and range of the parameters of the two-degree-of-freedom model fitted to individual apparent masses and phases are shown in Table 4B. The effect of intermittent random vibration compared to continuous random vibration on the model parameters has been investigated by comparing the parameters.

The primary segmental stiffness (k_1) was significantly greater ($p = 0.023$, Wilcoxon) with the intermittent signal than with the continuous signal at $1.0\,m\,s^{-2}$ rms (only subjects 1 and 12 showed the reverse trend), consistent with the characteristics of thixotropy. However, intermittency had no significant effect at $0.25\,m\,s^{-2}$ rms ($p = 0.695$, Wilcoxon, with six subjects having a higher k_1 with the intermittent signal and six having a higher k_1 with the continuous signal).

There was no significant difference in the secondary segmental stiffness (k_2) between the continuous and the intermittent stimulus at either $1.0\,m\,s^{-2}$ rms ($p = 0.084$, Wilcoxon) or $0.25\,m\,s^{-2}$ rms ($p = 0.754$, Wilcoxon). However, 10 of the 12 subjects showed a higher k_2 at $1.0\,m\,s^{-2}$ rms with the intermittent signal than with the continuous signal, consistent with thixotropy.

For the other parameters in the two-degree-of-freedom model, there were no significant differences between the continuous and the intermittent stimulus at either 0.25 or $1.0\,m\,s^{-2}$ rms.

3.2. Response in the horizontal (z-axis) cross-axis direction

3.2.1. Overview

The individual horizontal (z-axis) cross-axis apparent masses of the 12 subjects with the five magnitudes of continuous random vibration are shown in Fig. 8. The median normalised cross-axis apparent masses of the group of 12 subjects are shown in Fig. 9. The median and ranges of the individual peak frequencies are shown in Table 5. The individual horizontal cross-axis apparent masses of the 12 subjects with two vibration magnitudes (0.25 and $1.0\,m\,s^{-2}$ rms) with both continuous and intermittent random vibration are shown in Fig. 10.

The coherencies were generally lower than 0.5 with the lowest vibration magnitude ($0.125\,m\,s^{-2}$ rms) at frequencies less than 4.0–6.0 Hz. At $0.125\,m\,s^{-2}$ rms, the coherencies were generally in excess of 0.7 in the frequency range from about 6.0 Hz to between 14.0 and 16.0 Hz. At $1.0\,m\,s^{-2}$ rms, the coherencies were in excess of 0.8 in the frequency range from about 4.0 Hz to about 18.0 Hz.

There were three distinguishable peaks in each cross-axis apparent mass curve: the first below about 4.0–8.0 Hz, the second from around 4.0 or 8.0 Hz to around 12.0 Hz, the third between 14 and 16 Hz (Figs. 8 and 9). The third peak was caused by non-rigidity of the vibrator in the horizontal longitudinal direction during the vertical excitation. With no subject on the platform, the power spectral density of the measured horizontal acceleration showed a peak between 14 and 16 Hz with a magnitude less than 5% of the vertical acceleration excitation. The third peak was therefore excluded from further consideration. The first two peaks

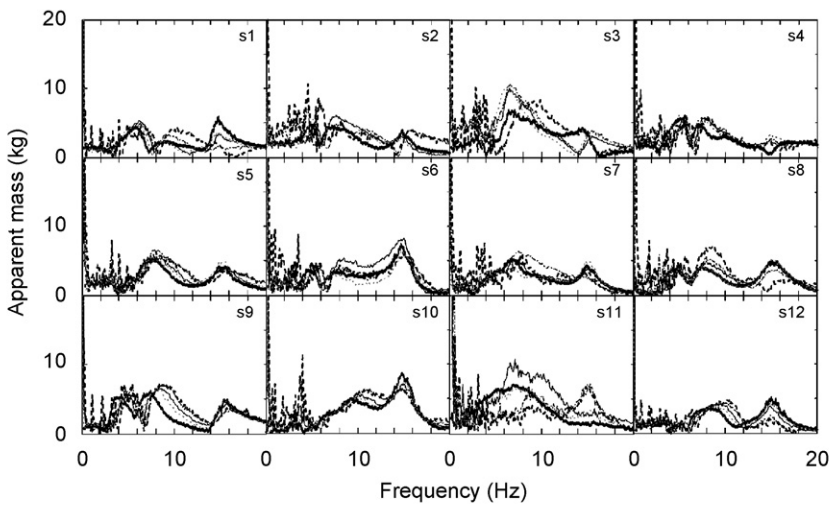

Fig. 8. Individual horizontal z-axis cross-axis apparent masses of 12 subjects (s1–s12) at five vibration magnitudes (- - - - - $0.125\,m\,s^{-2}$ rms; —·—·—·— $0.25\,m\,s^{-2}$ rms; ——— $0.5\,m\,s^{-2}$ rms; ········ $0.75\,m\,s^{-2}$ rms; ▬▬▬ $1.0\,m\,s^{-2}$ rms) of continuous random stimuli.

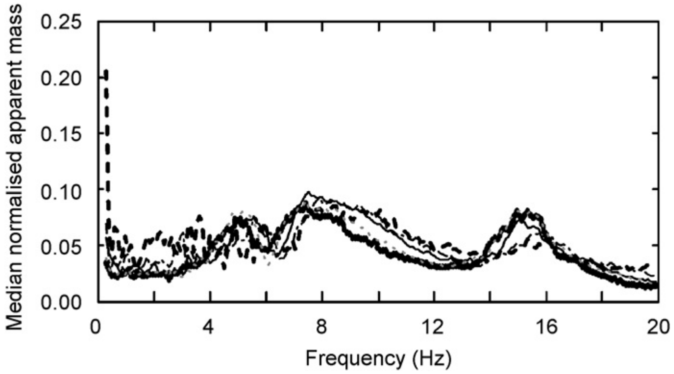

Fig. 9. Median normalised horizontal z-axis cross-axis apparent masses of the group of 12 subjects at five vibration magnitudes (- - - - - 0.125 m s^{-2} rms; —·—·—·—·— 0.25 m s^{-2} rms; ——— 0.5 m s^{-2} rms; ········· 0.75 m s^{-2} rms; ▬▬▬ 1.0 m s^{-2} rms) of continuous random stimuli.

Table 5
Median and ranges of peak frequencies of horizontal z-axis cross-axis apparent masses of 12 subjects at five vibration magnitudes (0.125, 0.25, 0.5, 0.75, and 1.0 m s^{-2} rms) of continuous random stimuli

(*A*) *Cross-axis peak frequencies of continuous random stimuli* (*Hz*)

Vibration magnitude (m s^{-2} rms)	Minimum	Median	Maximum
0.125	7.81	8.89	11.04
0.25	6.64	8.26	10.74
0.5	6.54	8.01	9.86
0.75	6.35	7.47	9.86
1.0	6.45	7.42	9.28

(*B*) *Cross-axis peak frequencies of intermittent random stimuli* (*Hz*)

Subject	0.25 m s^{-2} rms intermittent	0.25 m s^{-2} rms continuous	1.0 m s^{-2} rms intermittent	1.0 m s^{-2} rms continuous
s1	9.38	9.38	8.98	8.98
s2	8.20	8.20	7.03	7.03
s3	7.42	6.64	6.64	6.64
s4	7.81	7.81	7.42	7.03
s5	7.81	8.20	7.42	7.42
s6	7.81	8.59	7.42	7.81
s7	7.03	7.42	6.64	7.03
s8	8.20	8.20	7.42	7.81
s9	8.20	8.59	7.42	7.42
s10	10.55	11.33	9.77	9.38
s11	8.59	8.59	8.98	7.03
s12	9.78	9.38	8.98	8.20
Minimum	7.03	6.64	6.64	6.64
Median	8.20	8.40	7.42	7.42
Maximum	10.55	11.33	9.77	9.38

were caused by the biodynamic response of the human body and are of interest. The first peak had a low coherency (less than 0.3) below about 6.0 Hz, so the second peak was used to obtain the horizontal z-axis cross-axis apparent mass peak frequency as described in Section 2.5.3. The magnitudes of the horizontal z-axis cross-axis apparent masses at the peaks were less than 10% of the apparent masses at this frequency in the vertical direction.

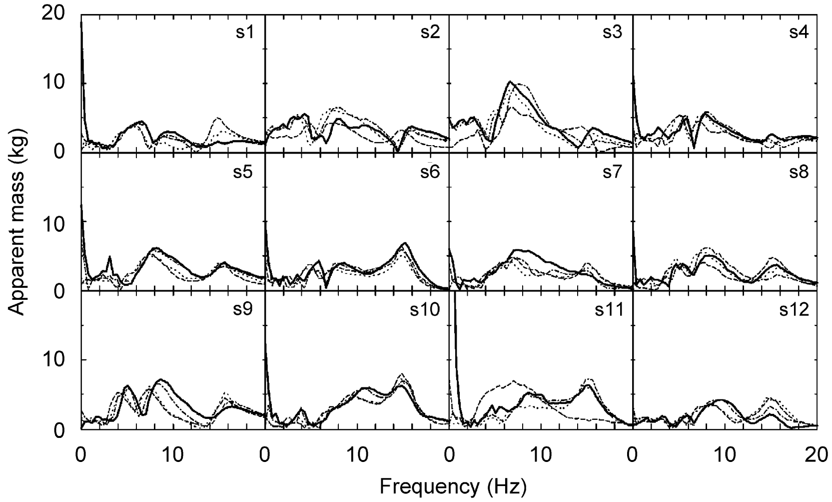

Fig. 10. Individual horizontal z-axis cross-axis apparent masses of 12 subjects (s1–s12) at two vibration magnitudes (—·—·—·— $0.25\,m\,s^{-2}$ rms intermittent; ········ $1.0\,m\,s^{-2}$ rms intermittent; ▬▬ $0.25\,m\,s^{-2}$ rms continuous; - - - - - $1.0\,m\,s^{-2}$ rms continuous) of both intermittent random stimuli and continuous random stimuli.

3.2.2. Horizontal (z-axis) cross-axis apparent mass peak frequencies with continuous random vibration

There was a significant effect of vibration magnitude on the horizontal (z-axis) cross-axis apparent mass peak frequencies ($p<0.01$, Friedman). The peak frequency decreased significantly with increasing vibration magnitude from 0.125 to $0.75\,m\,s^{-2}$ rms ($p<0.05$, Wilcoxon). There was no significant difference in the peak frequencies between 0.75 and $1.0\,m\,s^{-2}$ rms ($p = 0.14$, Wilcoxon).

The median peak frequencies of the cross-axis apparent masses of the 12 subjects decreased from 8.89 to 7.42 Hz as the vibration magnitude increased from 0.125 to $1.0\,m\,s^{-2}$ rms (Table 5A).

The peak frequencies of the median normalised cross-axis apparent masses of the group of 12 subjects were 8.40, 7.91, 7.52, 7.42, and 7.42 Hz with vibration magnitudes of 0.125, 0.25, 0.5, 0.75, and $1.0\,m\,s^{-2}$ rms, respectively (Fig. 9).

There were significant correlations between the cross-axis peak frequencies and the in-line resonance frequencies at $1.0\,m\,s^{-2}$ rms ($r = 0.858$, $p<0.01$, the Spearman rank order correlation test), $0.75\,m\,s^{-2}$ rms ($r = 0.785$, $p<0.01$, Spearman), $0.5\,m\,s^{-2}$ rms ($r = 0.835$, $p<0.01$, Spearman) and $0.25\,m\,s^{-2}$ rms ($r = 0.703$, $p = 0.011$, Spearman) $m\,s^{-2}$ rms. However, the correlation was not statistically significant at $0.125\,m\,s^{-2}$ rms ($r = 0.469$, $p = 0.124$, Spearman).

3.2.3. Horizontal (z-axis) cross-axis apparent mass peak frequencies with intermittent random vibration

The median peak frequency of the cross-axis apparent mass with intermittent random vibration decreased from 8.20 to 7.42 Hz as the vibration magnitude increased from 0.25 to $1.0\,m\,s^{-2}$ rms. With continuous random vibration, the median peak frequency decreased from 8.40 to 7.42 Hz as the vibration magnitude increased from 0.25 to $1.0\,m\,s^{-2}$ rms (Table 5B).

There was no significant difference between the peak frequency with $0.25\,m\,s^{-2}$ rms intermittent random vibration and the peak frequency with continuous random vibration at the same magnitude ($p = 0.257$, Wilcoxon). However, five subjects showed a lower peak frequency and only 2 subjects showed a higher peak frequency (five subjects showed no change) with intermittent stimuli than with continuous vibration at this magnitude (Fig. 10 and Table 5B). This implies that with some subjects the dynamic stiffness of the body in the horizontal cross-axis at the low magnitude was lowered due to prior high magnitude vibration in the vertical direction. At $1.0\,m\,s^{-2}$ rms, there was no significant difference between the peak frequency with intermittent random vibration and the peak frequency with continuous random vibration ($p = 0.705$, Wilcoxon).

The absolute differences between the peak frequencies at 0.25 and $1.0\,\mathrm{m\,s^{-2}}$ rms were marginally not significantly different between the intermittent random vibration and the continuous random vibration ($p = 0.095$, Friedman).

4. Discussion

4.1. Response in the vertical (x-axis) direction

4.1.1. Effect of the magnitude of continuous random vibration on apparent mass resonance frequency

The vertical in-line apparent masses at five magnitudes show that the semi-supine body is nonlinear: the resonance frequencies decreased significantly with increasing vibration magnitude. The relaxed semi-supine posture was assumed to involve less voluntary and involuntary muscular postural control of the body than sitting and standing postures used in most previous studies of the nonlinearity of the body. The consistent nonlinear response found here suggests that the nonlinearity is not primarily caused by active control of postural muscles but as a result of some passive property of the body (e.g. thixotropy) or, alternatively, an involuntary reflex response of the body.

A passive thixotropic characteristic implies that the dynamic stiffness of muscles, or other body components, undergoes a reduction as a result of mechanical perturbation, with a recovery after a period of stillness [17]. Fairley and Griffin [1] speculated that the nonlinear loosening effect of the musculo-skeletal structure had a similar mechanism to the thixotropic property of relaxed human muscles. However, there was no experimental data to support their hypothesis. The current study shows that the nonlinearity is present not only in postures where there is muscular control of posture but also in postures where muscular activity is not required to maintain posture. Previous studies with upright sitting and standing postures have found that variations in posture, so as to vary the muscular tension, have little effect on the nonlinearity. This is consistent with thixotropy rather than muscle activity being the primary cause of the nonlinearity.

The fore-and-aft apparent mass resonance frequency at the backrest for subjects sitting upright with average thigh contact while exposed to fore-and-aft random whole-body vibration reduced from 5 to 2 Hz (with normalised apparent mass at resonance between 1.5 and 1.2) as the vibration magnitude increased from 0.125 to $1.25\,\mathrm{m\,s^{-2}}$ rms [27]. Compared to that upright sitting posture with fore-and-aft excitation from the backrest, the semi-supine body exhibited higher equivalent stiffness (and a higher resonance frequency) but lower damping (indicated by the magnitude of the apparent mass at resonance). The lower resonance frequency of the fore-and-aft apparent mass on the backrest might be due to a pitching mode of the upper body pivoting upon the pelvic structure, whereas in the present study the response of the semi-supine body may be dominated by axial movement normal to the back in-line with the vertical x-axis excitation.

4.1.2. Effect of intermittency on apparent mass resonance frequency

The present results appear to be characteristic of thixotropic changes in the dynamic stiffness of the body during whole-body vibration: the resonance frequency at a low magnitude ($0.25\,\mathrm{m\,s^{-2}}$ rms) was lower with intermittent vibration than with the continuous vibration, whereas the resonance frequency at a high magnitude ($1.0\,\mathrm{m\,s^{-2}}$ rms) was higher with intermittent vibration than with continuous vibration. The resonance frequency at the low magnitude reflected the dynamic stiffness of the body 2.56 s after high magnitude 'perturbation'; the resonance frequency at the high magnitude reflected the dynamic stiffness of the body 2.56 s after low magnitude perturbation. With minimal postural muscle activity, the characteristics of the semi-supine body seem consistent with thixotropy being a cause of the characteristic nonlinearity, but the change found here was small and so if thixotropy is the primary cause of the nonlinearity it must have a time constant much less than 2.56 s.

A statistically significant variation in the stiffness of the body during the intermittent stimuli was only found for the stiffness of k_1 in the parametric model at $1.0\,\mathrm{m\,s^{-2}}$ rms (Section 3.1.5 and Table 4B). This suggests that the effect of the different shear histories on the dynamic stiffness of the body was small, or that the body stiffness recovered very quickly after perturbation, for example in less than 2.56 s.

The nonlinearity in steady-state sitting conditions have been found to be significantly reduced by some periodic muscle activity associated with voluntary body movement, with the reduction mainly due to a change in the resonance frequency with low magnitudes of vibration [16]. With normal steady-state sitting, the biodynamic response of the body may be influenced by voluntary muscular control of posture in response to the vibration, by involuntary muscular reflex responses, and by the passive dynamic property of muscles and tissues (including thixotropy). In addition to these three components, voluntary periodic movement involves muscular control. If the passive thixotropy of tissues is a cause of the nonlinearity and if voluntary periodic muscular activity has the same effect on the thixotropy at low and at high magnitudes of vibration, the resonance frequencies might be expected to decrease at both low and high magnitudes. However, voluntary periodic muscular activity was more effective in reducing the resonance frequency at low magnitudes, suggesting that the voluntary movement had a different effect on thixotropy at different magnitudes of vibration. At high magnitudes of vibration, the passive deformation and shearing stress on muscles and other tissues from the vibration may have already reduced the dynamic stiffness, so that the effect of voluntary muscle activity on dynamic stiffness was less at higher vibration magnitudes.

Thixotropy is a passive response of the body and muscle reflex responses are involuntary. During whole-body vibration, both responses could be present in the relaxed semi-supine body. Neuromuscular reflex responses are a necessary component in the control of spinal stability [28], and by measuring trunk muscle EMG [29] reflex responses of paraspinal muscles have been found associated with movement disturbances. Possibly, with low magnitudes of vibration, involuntary muscular reflex response may increase the dynamic stiffness of the body, whereas at high magnitudes the relative contribution from reflex response may be less than the contribution with low magnitudes of vibration, resulting in a softer body at higher magnitudes. The relaxed semi-supine conditions of the present study allowed the subjects to lie with minimal voluntary and involuntary muscular activity, or at least, less voluntary and involuntary muscular activity than when sitting and standing. The consistent nonlinear response with relaxed passive body tissues suggests muscle activity may not be the primary cause of the nonlinearity.

4.2. Response in the horizontal z-axis cross-axis direction

4.2.1. Effect of the magnitude of continuous random vibration on horizontal z-axis cross-axis apparent mass peak frequencies

The peak frequencies of the horizontal z-axis cross-axis apparent masses were significantly correlated with the resonance frequencies of the vertical x-axis in-line apparent masses at four (0.25, 0.5, 0.75, and 1.0 $\mathrm{m\,s^{-2}}$ rms) of the five vibration magnitudes (Section 3.2.2). This may suggest that the responses in the two axes are cross-coupled by a common mechanism. The horizontal z-axis cross-axis apparent masses at five magnitudes also show that the semi-supine body is nonlinear: the peak frequency decreased significantly with increasing vibration magnitude. The consistent nonlinear response in both the vertical x-axis and horizontal z-axis suggests the nonlinearities in these two directions may have a common cause.

Using upright sitting posture with a backrest and minimal thigh contact, Nawayseh and Griffin [27] found that the dominant vertical z-axis cross-axis apparent mass peak frequency at the back during fore-and-aft x-axis whole-body vibration was in the range 5–7 Hz at vibration magnitudes between 0.625 and 0.125 $\mathrm{m\,s^{-2}}$ rms This frequency range differed from the resonance frequencies in the fore-and-aft in-line direction at the back while seated (i.e., 3–5 Hz). The magnitude of the vertical cross-axis forces present on the backrest was small (less than 4 kg at the peak). The authors explained that the expected magnitudes of rotational modes in the mid-sagittal plane of the head, the spine and the pelvis were reduced by some vertical motion of the spine counteracting the pitching motions. In the present study, the horizontal cross-axis peak frequencies were in the range 7–9 Hz which coincides with the vertical in-line resonance frequency between 7 and 10 Hz, suggesting common modes in the vertical in-line and horizontal cross-axis responses. The magnitude of the cross-axis apparent mass of the semi-supine body is also small in the present study (up to 5 kg at peak and less than 10% of the vertical in-line apparent mass at resonance).

4.2.2. Effect of intermittent random stimuli on z-axis cross-axis apparent mass peak frequencies

The apparent dependence of the response on the shear history in the vertical in-line response was not significant in the cross-axis direction. This could be due to a lower magnitude of cross-axis response and less nonlinearity presented in the cross-axis than in the vertical direction. The magnitudes of the cross-axis apparent masses are less than 10% of the vertical in-line apparent masses—the maximum values of the median normalised apparent mass and the median normalised cross-axis apparent mass were 1.60 and 0.10, respectively (Fig. 10). The absolute difference between the peak frequencies of the median normalised cross-axis apparent masses at $0.125\,m\,s^{-2}$ rms (8.40 Hz) and at $1.0\,m\,s^{-2}$ rms (7.42 Hz) was 0.98 Hz. The absolute difference for the vertical in-line apparent mass was 3.03 Hz (10.35 Hz at $0.125\,m\,s^{-2}$ rms and 7.32 Hz at $1.0\,m\,s^{-2}$ rms). On this basis, the nonlinearity in the cross-axis direction was only 32% (0.98/3.03 Hz) of the nonlinearity in the vertical direction.

5. Conclusions

With minimal voluntary and involuntary muscular activity, the relaxed semi-supine body showed a consistent nonlinear biodynamic response, both in the vertical (x-axis) direction and in the horizontal (z-axis) cross-axis direction, during vertical whole-body vibration.

The responses of the semi-supine body during intermittent random vibration had a typical thixotropic characteristic at both a low magnitude of vibration ($0.25\,m\,s^{-2}$ rms) and a high magnitude of vibration ($1.0\,m\,s^{-2}$ rms). This resulted in less nonlinearity than with continuous random vibration. It is concluded that the passive thixotropic properties of the body could be the principal cause of the nonlinearity seen in measures of the apparent mass and transmissibility of the human body.

References

[1] T.E. Fairley, M.J. Griffin, The apparent mass of the seated human body: vertical vibration, *Journal of Biomechanics* 22 (2) (1989) 81–94.
[2] N.J. Mansfield, M.J. Griffin, Non-linearities in apparent mass and transmissibility during exposure to whole-body vertical vibration, *Journal of Biomechanics* 33 (2000) 933–941.
[3] N.J. Mansfield, M.J. Griffin, Effects of posture and vibration magnitude on apparent mass and pelvis rotation during exposure to whole-body vertical vibration, *Journal of Sound and Vibration* 253 (1) (2002) 93–107.
[4] Y. Matsumoto, M.J. Griffin, Non-linear characteristics in the dynamic responses of seated subjects exposed to vertical whole-body vibration, *Journal of Biomechanical Engineering* 124 (2002) 527–532.
[5] N. Nawayseh, M.J. Griffin, Non-linear dual-axis biodynamic response to vertical whole-body vibration, *Journal of Sound and Vibration* 268 (2003) 503–523.
[6] T.E. Fairley, M.J. Griffin, The apparent mass of the seated human body in the fore-and-aft and lateral directions, *Journal of Sound and Vibration* 139 (2) (1990) 299–306.
[7] N.J. Mansfield, R. Lundström, The apparent mass of the human body exposed to non-orthogonal horizontal vibration, *Journal of Biomechanics* 32 (1999) 1269–1278.
[8] P. Holmlund, R. Lundström, Mechanical impedance of the sitting human body in single-axis compared to multi-axis whole-body vibration exposure, *Clinical Biomechanics* 16 (Suppl. 1) (2001) S101–S110.
[9] N. Nawayseh, M.J. Griffin, Non-linear dual-axis biodynamic response to fore-and-aft whole-body vibration, *Journal of Sound and Vibration* 282 (2005) 831–862.
[10] N.A. Abdul Jalil, Transmission of Vibration Through Backrests and Apparent Mass of the Back During Whole-Body Fore-and-Aft Vibration, PhD Thesis, University of Southampton, 2006.
[11] Y. Matsumoto, M.J. Griffin, Dynamic response of the standing human body exposed to vertical vibration: influence of posture and vibration magnitude, *Journal of Sound and Vibration* 212 (1) (1998) 85–107.
[12] G.H.M.J. Subashi, Y. Matsumoto, M.J. Griffin, Apparent mass and cross-axis apparent mass of standing subjects during exposure to vertical whole-body vibration, *Journal of Sound and Vibration* 293 (1–2) (2006) 78–95.
[13] Y. Matsumoto, M.J. Griffin, Effect of muscle tension on non-linearities in the apparent masses of seated subjects exposed to vertical whole-body vibration, *Journal of Sound and Vibration* 253 (1) (2002) 77–92.
[14] C.D. Robertson, M.J. Griffin, Laboratory studies of the electromyographic response to whole-body vibration, ISVR Technical Report 184, 1989, University of Southampton.
[15] R. Blüthner, H. Seidel, B. Hinz, Myoelectric response of back muscles to vertical random whole-body vibration with different magnitudes at different postures, *Journal of Sound and Vibration* 253 (1) (2002) 37–56.
[16] Y. Huang, M.J. Griffin, Effect of voluntary periodic muscular activity on nonlinearity in the apparent mass of the seated human body during vertical random whole-body vibration, *Journal of Sound and Vibration* 298 (2006) 824–840.
[17] M. Lakie, Vibration causes stiffness changes (thixotropic behaviour) in relaxed human muscle, *United Kingdom Group Informal Meeting on Human Response to Vibration*, Loughborough University of Technology, 22–23 September 1986.
[18] M. Lakie, E.G. Walsh, G.W. Wright, Passive wrist movements—a large thixotropic effect, *Journal of Physiology* 300 (1979) 36–37.

[19] K.E. Hagbarth, J.V. Hagglund, M. Nordin, E.U. Wallin, Thixotropic behaviour of human finger flexor muscles with accompanying changes in spindle and reflex responses to stretch, *Journal of Physiology, London* 368 (1985) 323–342.

[20] I. Homma, K.E. Hagbarth, Thixotropy of rib cage respiratory muscles in normal subjects, *Journal of Applied Physiology* 89 (2000) 1753–1758.

[21] N.J. Mansfield, Non-linear Dynamic Response of the Seated Person to Whole-Body-Vibration, PhD thesis, University of Southampton, 1998.

[22] L.H. Vogt, H.E. Krause, H. Hohlweck, E. May, Mechanical impedance of supine humans under sustained acceleration, *Aerospace Medicine* 44 (2) (1973) 123–128.

[23] L.H. Vogt, H. Mertens, H.E. Krause, Model of the supine human body and its reactions to external forces, *Aviation, Space, and Environmental Medicine* 49 (1) (1978) 270–278.

[24] J.Z. Liu, M. Kubo, H. Aoki, F. Terauchi, The transfer function of human body on vertical sinusoidal vibration, *The Japanese Journal of Ergonomics* 32 (1) (1996) 29–38.

[25] H.C. Vykukal, Dynamic response of the human body to vibration when combined with various magnitudes of linear acceleration, *Aerospace Medicine* 39 (1968) 1163–1166.

[26] L. Wei, M.J. Griffin, Mathematical models for the apparent mass of the seated human body exposed to vertical vibration, *Journal of Sound and Vibration* 212 (5) (1998) 855–874.

[27] N. Nawayseh, M.J. Griffin, Tri-axial forces at the seat and backrest during whole-body fore-and-aft vibration, *Journal of Sound and Vibration* 281 (2005) 921–942.

[28] K.M. Moorhouse, K.P. Granata, Role of reflex dynamics in spinal stability: intrinsic muscle stiffness alone is insufficient for stability, *Journal of Biomechanics* 40 (5) (2007) 1058–1065.

[29] K.P. Granata, G.P. Slota, B.C. Bennett, Paraspinal muscle reflex dynamics, *Journal of Biomechanics* 37 (2004) 241–247.